Oikos

OIK-07073

Herberich, M. M., Gayler, S., Anand, M. and Tielbörger, K. 2020. Biomass–density relationships of plant communities deviate from the self-thinning rule due to age structure and abiotic stress. – Oikos doi: 10.1111/oik.07073

Appendix 1

Supplementary information concerning PLANTHeR model description

A detailed model description of PLANTHeR following as well as a model plausibility analysis is found in Herberich et al. (2017). The model design including the parameter values (Appendix 2) are the same as in Herberich et al. (2017), and thus we only give a brief model description following the ODD (Overview, Design concepts, Details, (Grimm et al. 2006, 2010)) protocol here. The category 'Overview' and the element 'Initialization' can be found in the main body of the paper. Elements of the ODD protocol which are not represented in PLANTHeR are not addressed.

1.1 Design concepts

1.1.1. Basic principles

Seeds do not compete with adult plants for water. This is because 1) viable dormant seeds generally have a low water content and do not absorb water actively during the growing season, and 2) only the micro-climatic conditions in the intermediate vicinity of the seed determine the seed fate (Mayer and Poljakoff-Mayber 1982).

Only one individual can grow per cell which imposes a carrying capacity on the system.

The model was designed by pattern-oriented modelling at both the individual level (sigmoidal plant growth, growth dependent mortality, etc.), and the system level (changes in the size structure of the population or community) (Grimm et al. 2005).

1.1.2. Emergence

The observed biomass–density relationships through time emerged from local interactions, complete life cycles of individuals and the soil water potentials.

1.1.3. Sensing

Individuals sense the soil water potentials and other individuals present in their Zone of Influence.

1.1.4. Interactions

Individuals interact directly by means of competition for available soil water (Appendix 1, 1.2.1) and for vacant positions (Appendix 1, 1.2.4).

1.1.5. Stochasticity

Stochasticity is included in the initialization of the plant community (2.1.3), the seed survival (Appendix 1, 1.2.2), the germination (Appendix 1, 1.2.3), the seedling establishment (Appendix 1, 1.2.4), the seed dispersal (Appendix 1, 1.2.6), and perennial mortality (Appendix 1, 1.2.7).

A1.6. Observation

A summary output file reports community status at the end of each time step. The summary includes the total community size, the number and summed ZOI of individuals per PFT, PFT richness, and Shannon diversity index.

An additional file recorded the number of individuals and their biomass at the end of each time step.

1.2. Submodels

1.2.1. Soil water uptake

Non-optimal soil water conditions limit plant performance. This is simulated by means of a reduction function f(Ψ), a dimensionless prescribed function of the soil water potential Ψ [mm] based on four critical values Ψ_1 - Ψ_{PWP} (Feddes et al. 1978). Water uptake below $|\Psi_1|$ (oxygen deficiency (Yang and Jong 1971)) and above $|\Psi_{PWP}|$ (permanent wilting point) is set to zero (equation 4). Between $|\Psi_2|$ and $|\Psi_3|$ water conditions are optimal. Between $|\Psi_1|$ and $|\Psi_2|$ and between $|\Psi_3|$ and $|\Psi_{PWP}|$ a linear relationship is assumed.

$$f(\Psi) \begin{cases} 0 & \text{if } \Psi < \Psi_{PWP} \\ \frac{\Psi - \Psi_{PWP}}{\Psi_3 - \Psi_{PWP}} & \text{if } \Psi_{PWP} \leq \Psi < \Psi_3 \\ 1 & \text{if } \Psi_3 \leq \Psi < \Psi_2 \\ \frac{\Psi_1 - \Psi}{\Psi_1 - \Psi_2} & \text{if } \Psi_2 \leq \Psi < \Psi_1 \\ 0 & \text{if } \Psi_1 \leq \Psi \end{cases} \quad \text{(A1)}$$

Values of Ψ_1 - Ψ_{PWP} were chosen so that the reduction functions for high ($f_T(\Psi)$) and low water stress tolerant PFTs ($f_t(\Psi)$) differed maximally (Table A1) (Wesseling 1991, Bittner et al. 2010, Herberich et al. 2017). Thereby, high water stress tolerance signifies high tolerance to dry but low tolerance to wet conditions and *vice-versa* for low water stress tolerance.

Table A1.1. Critical potentials Ψ_i [mm] governing the reduction function for PFTs with high water stress tolerance ($f_T(\Psi)$) and low water stress tolerance ($f_t(\Psi)$).

Ψ_i	Water stress tolerance high	Water stress tolerance low
Ψ_1	-150	-1
Ψ_2	-300	-10
Ψ_3	-10000	-2000
Ψ_{PWP}	-240000	-80000

Individuals can acquire water within and beyond the cell in which they are positioned following the distance-dependent Zone of Influence (ZOI) modelling approach (Czárán 1998). The number of individuals that can overlap with their ZOI is theoretically unlimited. Individuals compete with neighbors solely in areas of ZOI overlap. Competition for water is size-symmetric due to the non-pre-emptable uniform distribution of water (Schulte et al. 2013). Here, we simulate completely size-symmetric competition (Weiner and Damgaard 2006):

$$E(\Psi)_{i(x,y)} = \frac{f_i(\Psi)_{(x,y)}}{N_{(x,y)}} \quad \text{(A2)}$$

Where $E(\Psi)_{i(x,y)}$ represents the effective amount of water available to individual i of cell (x,y), $f_i(\Psi)$ is the reduction function of individual i in cell (x,y), and $N_{(x,y)}$ is the total number of individuals with cell (x, y) in their ZOI.

The total water availability of an individual i, F_Ψ, is calculated as the average value of $E(\Psi)_i$ over the number of cells within the individual's ZOI C:

$$F_\Psi = \sum_{(x,y)\in \text{ZOIi}} \frac{E(\Psi)_{i,(x,y)}}{C} \quad \text{(A3)}$$

We assume that when $F_\Psi = 0$, water availability can immediately increase above 0 as soon as $\Psi_{PWP} < \Psi < \Psi_1$ regardless of the duration of periods where F_Ψ equals zero.

1.2.2. Seed survival in the seed bank

Seed viability was drawn from a normal distribution truncated between 0 years and 100 years with a mean seed viability of 10 years and SD of 5 years (Roberts 1972). This resulted in a long-term seed bank with seeds persisting in the soil for at least five years, similar to most plant species regularly found in seed banks (Bakker et al. 1996).

1.2.3. Germination

In each year, germination probability is individually calculated for each seed based on its functional trait value for seed dormancy multiplied with its PFT specific reduction function f(Ψ) (Levitt 1980). Seeds remain in the seed bank until they die or germinate.

1.2.4. Seedling establishment

Only a single individual can establish per empty cell. Seedling establishment is modelled as a weighted lottery where the probability for a seed to establish is determined by its competitive ability and life form. Specifically, annuals have a 2:1 chance to establish based on the general assumption that annuals are better colonizers of newly opened gaps (DiVittorio et al. 2007, Seifan et al. 2012).

1.2.5. Adult growth

A plant's aboveground dry biomass [mg], B, is allometrically related to its area [cm^2], ZOI, as ZOI ~ $\mu B^{2/3}$ with the proportionality constant $\mu = 1$ (Weiner et al. 2001). Adult growth is modelled as the annual increase of an individual's ZOI radius, r:

$$r_{(t+1)} = r_t + G \times F_\Psi \times \left(1 - \frac{r_t}{r_{max}}\right) \quad \text{(A4)}$$

where F_Ψ is the total water availability of an individual (Appendix 1, 1.2.1.), t is the individual's age, and G is the PFT's specific maximum adult growth rate. The choice of the maximum ZOI radius, r_{max}, depends on the studied ecosystem. Here, we fixed it at 5 m to approximate the ZOI radius of a large tree canopy (Caplat and Anand 2009).

1.2.6. Seed production and dispersal

Minimum and maximum seed numbers are equal for all PFTs [1; 20] (Bauer et al. 2002, Snyder 2011). The actual number of produced viable seeds, S, is calculated using a Gompertz function:

$$S = 20 \times e^{\left(\ln\frac{1}{20}\right)e^{(-k \times I)}} \times F_\Psi \quad \text{(A5)}$$

where k = 1 [1/cm], and I is the annual ZOI increment [cm]. Seeds are classified by their position, age and PFT but not their size. Consequently, different PFTs may produce a similar number of assumedly similar sized seeds given a comparable I and F_Ψ. This means that the PFTs are on the same point on the surface of the trade-off between seed number and seed size (Jakobsson and Eriksson 2000).

Seeds inherit their PFT identity from their parent plant but differ in their exact functional trait values which are drawn for each individual separately (Sect. 2.1). For each seed, the dispersal distance is determined from a log-normal dispersal kernel with the PFT's specific value as a mean (Stoyan and Wagner 2001). We assume no directed dispersal.

1.2.7. Adult mortality

Mortality due to water stress was calculated for both annuals and perennials based on mean total water availability of an individual F_Ψ (Appendix 1, 1.2.1.) over the growing season. Most higher plants die after losing 60% to 90% of their water content, therefore individuals were assigned dead when their mean F_Ψ fell below 0.1 (Levitt 1980).

Perennial mortality probability, m, is a function of natural senescence (Caplat et al. 2008):

$$m = M_0 \times e^{-M_d \times I} \quad \text{(A6)}$$

where M_0 = 0.8 is the probability of mortality at zero growth, M_d = 0.08 the decay rate of growth dependent mortality [1/cm], and I is the annual ZOI increment [cm]. All annuals die at the end of each time step.

Appendix 2

Supplementary information on PFT parametrization and model parameters

Table A2.1. Functional trait strategies and their specific parameter values or trait syndromes.

Functional trait	Mean value or trait syndrome of functional trait strategy with the capital letter	Mean value or trait syndrome of functional trait strategy with the lowercase letter	Unit
Seedling competitive ability	80	20	%
Maximum adult growth rate	80	20	%
Seed dormancy	80	20	%
Seed dispersal distance	16	4	m
Life form	perennial	annual	category
Ψ_1	- 150	- 1	mm
Ψ_2	- 300	- 10	mm
Ψ_3	- 10000	- 2000	mm
Ψ_{PWP}	- 240000	- 80000	mm

Note. - PLANTHeR includes six rather general, composite functional traits that can represent several substitutional traits depending on the specific ecosystem. These traits are seedling competitive ability, maximum adult growth rate, seed dormancy, seed dispersal distance, life form, and water stress tolerance. Each functional trait is represented by two opposing strategies: perennial(P)/annual(a) life form, high(T)/low(t) water stress tolerance, long(D)/short(d) seed dispersal distance, long-(S)/short-term(s) seed dormancy, strong(C)/weak(c) seedling competitive ability, and high(G)/low(g) maximum adult growth rate (Seifan et al. 2012, Seifan et al. 2013). Differences in water stress tolerance are simulated by the means of a reduction function f(Ψ), a dimensionless prescribed function of the soil water potential Ψ [mm] based on four critical values $\Psi_1 - \Psi_{PWP}$ (Feddes et al. 1978). (Herberich et al. 2017)

Table A2.2. Overview of the model parameters and default values used in the present analysis.

Level	Parameter and its description	Value	Unit	Reference
Domain	Number of cells	640000		
	Cell size	25	cm^2	(Schippers et al. 2001)
Individual	Mean seed viability	10	years	(Bakker et al. 1996)
	Maximum radius of the zone of influence, r_{max}	5	m	(Caplat and Anand 2009)
	Probability of mortality at zero growth, M_0	0.8		(Caplat et al. 2008)
	Decay rate of growth dependent mortality, M_d	0.08	1/cm	(Caplat et al. 2008)
	Threshold level for mortality due to water stress, i.e. minimum mean F_Ψ	0.1		(Levitt 1980)
	Maximum seed amount	20		(Bauer et al. 2002); (Snyder 2011)
	Minimum seed amount	1		

Table A2.3. 64 modelled PFTs in the plant community which resulted from full factorial combinations of two opposing strategies of the six traits. Functional trait strategies were: perennial(P)/annual(a) life form, high(T)/low(t) water stress tolerance, long(D)/short(d) seed dispersal distance, long-(S)/short-term(s) seed dormancy, strong(C)/weak(c) seedling competitive ability, and high(G)/low(g) maximum adult growth rate. Except for the functional traits life form and water stress tolerance, the functional trait strategy indicated by the capital letter stands for 80% of the maximum trait value whereas the strategy indicated by the lowercase letter stands for 20%, respectively. A "jack-of-all-trades, master-of-nothing" PFT, i.e., 50% of maximum values for all traits is not included in the simulations. High(T)/low(t) water stress tolerance is simulated by means of different reduction functions f(Ψ), dimensionless prescribed functions of the soil water potential Ψ [mm] based on four critical values Ψ_1 - Ψ_{PWP} (Feddes et al. 1978). Thereby, high water stress tolerance signifies high tolerance to dry but low tolerance to wet conditions and vice-versa for low water stress tolerance. Thus, PFT 63 (PTDSCG) is not a so-called "Darwinian demon" because it has a low tolerance to excessive water availability. (from Herberich et al. 2017)

Plant functional type	Life form perennial (P) / annual (a)	Water stress tolerance high (T) / low (t)	Maximum seed dispersal distance long (D) / short (d)	Seed dormancy long- (S) / short-term (s)	Competitive ability strong (C) / weak (c)	Maximum growth rate high (G) / low (g)
PFT1	P	T	D	S	C	g
PFT2	P	T	D	S	c	G
PFT3	P	T	D	S	c	g
PFT4	P	T	D	s	C	G
PFT5	P	T	D	s	C	g
PFT6	P	T	D	s	c	G
PFT7	P	T	D	s	c	g
PFT8	P	T	d	S	C	G
PFT9	P	T	d	S	C	g
PFT10	P	T	d	S	c	G
PFT11	P	T	d	S	c	g
PFT12	P	T	d	s	C	G
PFT13	P	T	d	s	C	g
PFT14	P	T	d	s	c	G
PFT15	P	T	d	s	c	g
PFT16	P	t	D	S	C	G
PFT17	P	t	D	S	C	g
PFT18	P	t	D	S	c	G
PFT19	P	t	D	S	c	g
PFT20	P	t	D	s	C	G
PFT21	P	t	D	s	C	g
PFT22	P	t	D	s	c	G
PFT23	P	t	D	s	c	g
PFT24	P	t	d	S	C	G
PFT25	P	t	d	S	C	g
PFT26	P	t	d	S	c	G
PFT27	P	t	d	S	c	g
PFT28	P	t	d	s	C	G
PFT29	P	t	d	s	C	g
PFT30	P	t	d	s	c	G
PFT31	P	t	d	s	c	g

PFT32	a	T	D	S	C	G
PFT33	a	T	D	S	C	g
PFT34	a	T	D	S	c	G
PFT35	a	T	D	S	c	g
PFT36	a	T	D	s	C	G
PFT37	a	T	D	s	C	g
PFT38	a	T	D	s	c	G
PFT39	a	T	D	s	c	g
PFT40	a	T	d	S	C	G
PFT41	a	T	d	S	C	g
PFT42	a	T	d	S	c	G
PFT43	a	T	d	S	c	g
PFT44	a	T	d	s	C	G
PFT45	a	T	d	s	C	g
PFT46	a	T	d	s	c	G
PFT47	a	T	d	s	c	g
PFT48	a	t	D	S	C	G
PFT49	a	t	D	S	C	g
PFT50	a	t	D	S	c	G
PFT51	a	t	D	S	c	g
PFT52	a	t	D	s	C	G
PFT53	a	t	D	s	C	g
PFT54	a	t	D	s	c	G
PFT55	a	t	D	s	c	g
PFT56	a	t	d	S	C	G
PFT57	a	t	d	S	C	g
PFT58	a	t	d	S	c	G
PFT59	a	t	d	S	c	g
PFT60	a	t	d	s	C	G
PFT61	a	t	d	s	C	g
PFT62	a	t	d	s	c	G
PFT63	P	T	D	S	C	G
PFT64	a	t	d	s	c	g

Appendix 3

Supplementary information about community diversity and simulation time

The goal of this study was to disentangle the effects of age-structure, functional diversity and abiotic stress on the biomass–density trajectory of plant communities. To ensure that the number of sections of the biomass–density trajectory were not a function of the simulation time, we compared PFT richness and Shannon diversity index every 100 years along the complete simulation runs (2000 years) (Herberich et al. 2017). Using these comparisons, we could detect the time scale at which the functional structure of the community stopped changing significantly ($p > 0.05$, see figure caption below).

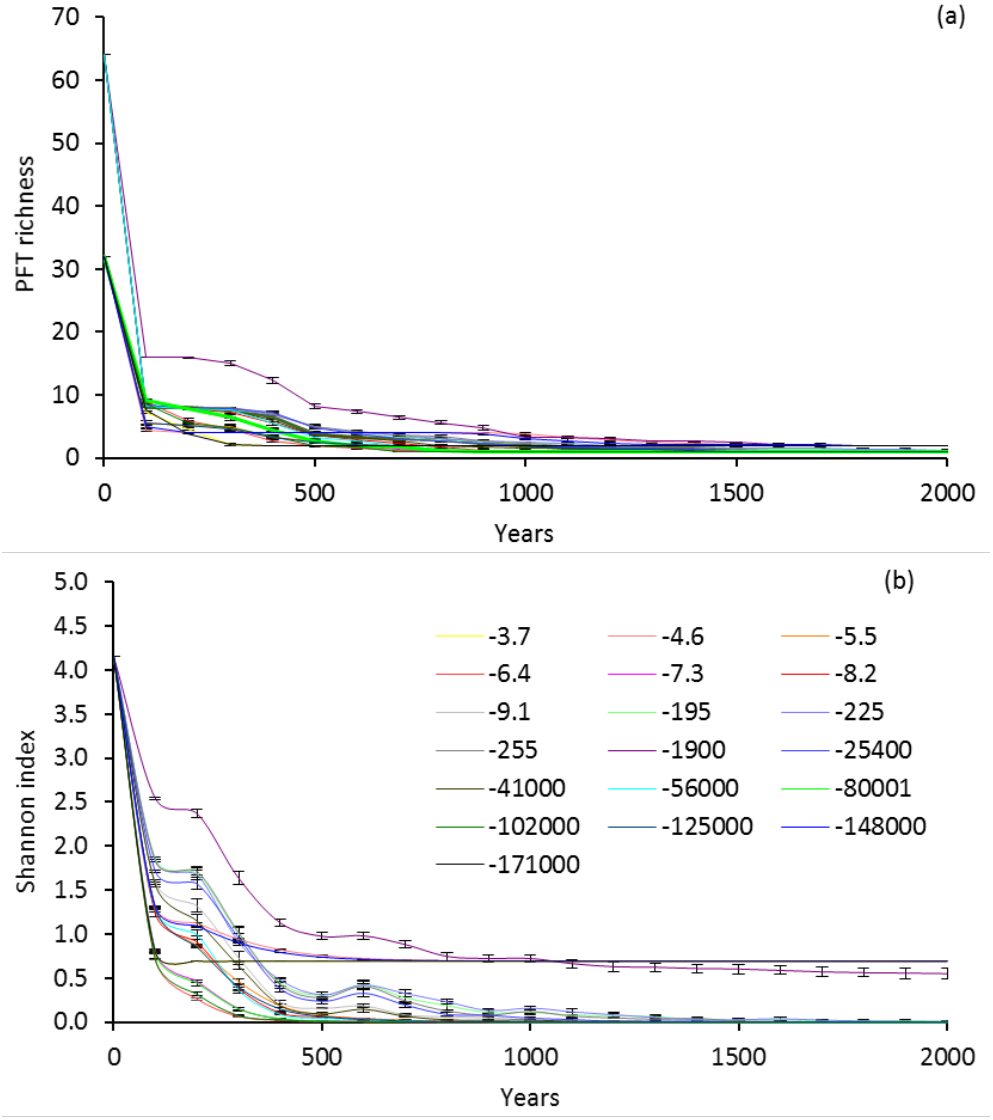

Figure A3.1. Adapted from Herberich et al. (2017). Change in mean ± SD PFT richness (a) and Shannon diversity index (b) of ten replicated model runs of 2000 years each. Nineteen soil water potentials [mm] were modelled, respectively. PFT richness and Shannon diversity index were generally consistent in their decreasing trend in time, however, these two measures did not stabilize at the exact point in time for all soil water potentials. PFT richness stabilized latest after 1500 years, meaning that we did not find any significant differences ($p > 0.05$) among the soil water potentials in PFT richness after 1500 years. On the other hand, the values of the Shannon diversity index stabilized already latest after 1100 years for all soil water potentials. Therefore, we conclude that the simulation time used for the analyses (2000 years) captured a stable adjustment of the plant community to the specific soil water potentials.

Appendix 4

Biomass–density trajectories and skewness of the biomass distribution for all 19 soil water scenarios.

Changes in the biomass–density trajectory over time can be tracked by means of the skewness of the biomass distribution (Berger et al. 2002). Here, the skewness of the biomass distribution subdivided the biomass–density trajectory into maximum four distinct sections. Section I (blue) was characterized by an increase of positive skewness and ended with the first maximum of skewness. Section II (orange) was characterized by a constant decrease of positive skewness between the first maximum and the first x-intercept. Section III (yellow) was characterized by a negative skewness between the two x-intercepts. Section IV (green) started at the second x-intercept with an increasing positive skewness and was characterized by alternating phases of increasing and decreasing skewness.

Figures D1 to D15 show for all nineteen soil water scenarios: (a) Entire biomass–density trajectory, i.e. relationship between the logarithm of mean plant biomass of survivors w (mg/m²) and the logarithm of plant density N (individuals/m²) for all ten replicate model runs over 2000 years. Colors show the four sections indicated by the skewness of the biomass distribution in Fig. b. The steeper dotted line has a slope of - 3/2 and the flat dashed line has a slope of -1.1. (b) Change in mean ± SD (in grey) skewness of biomass distribution across ten replicates over 2000 years.

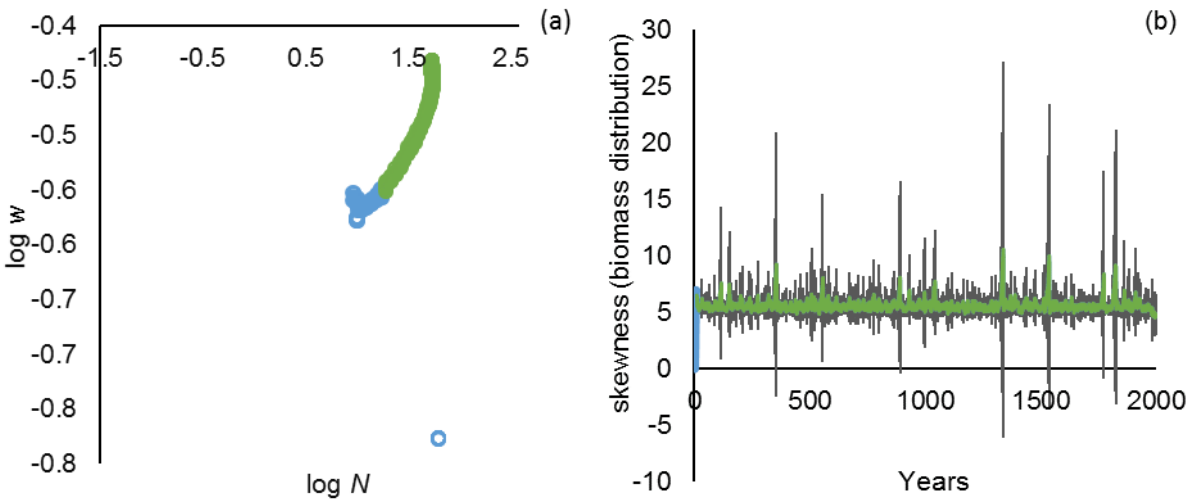

Figure A4.1. Soil water potential -171000, $f_d(\Psi) = 0.30$.

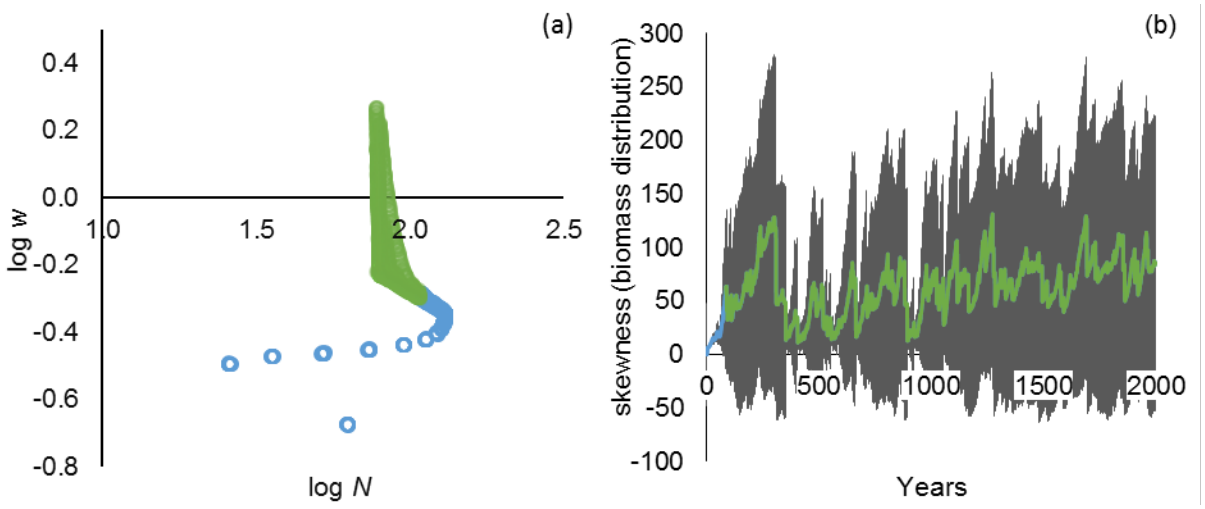

Figure A4.2. Soil water potential -148000, $f_d(\Psi) = 0.40$.

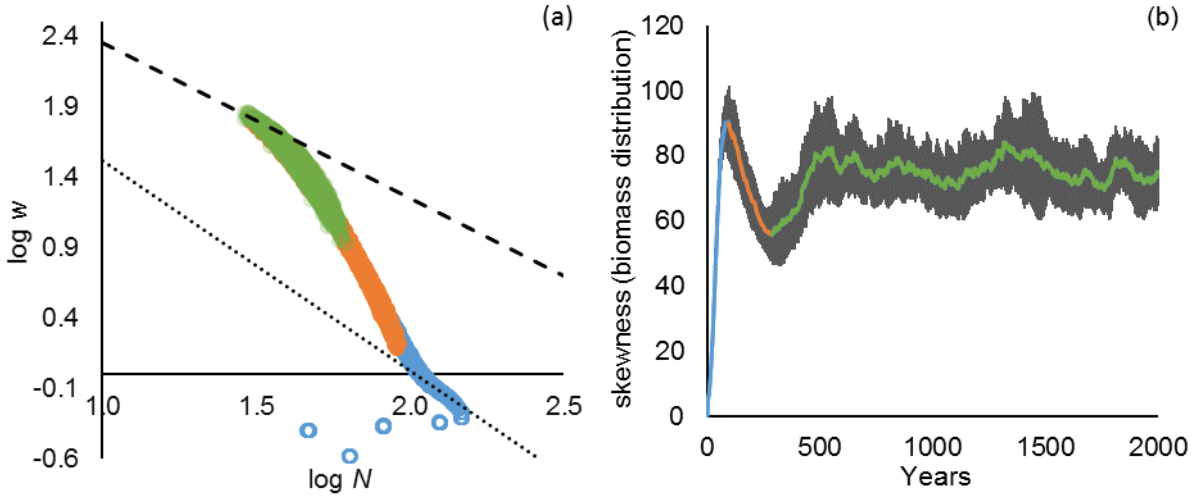

Figure A4.3. S Soil water potential -125000, $f_d(\Psi) = 0.50$.

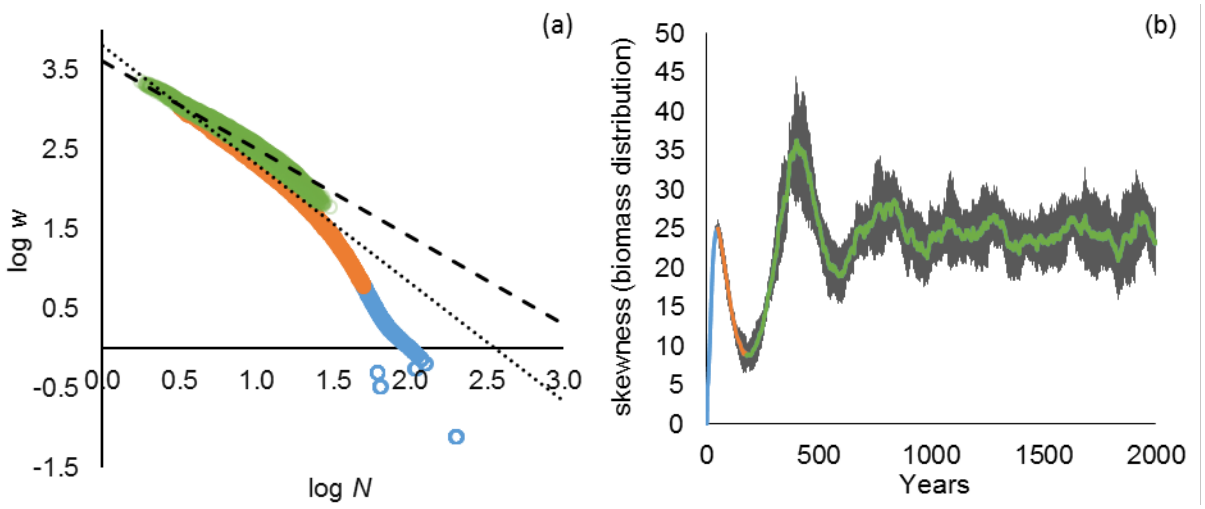

Figure A4.4. S Soil water potential -102000, $f_d(\Psi) = 0.60$.

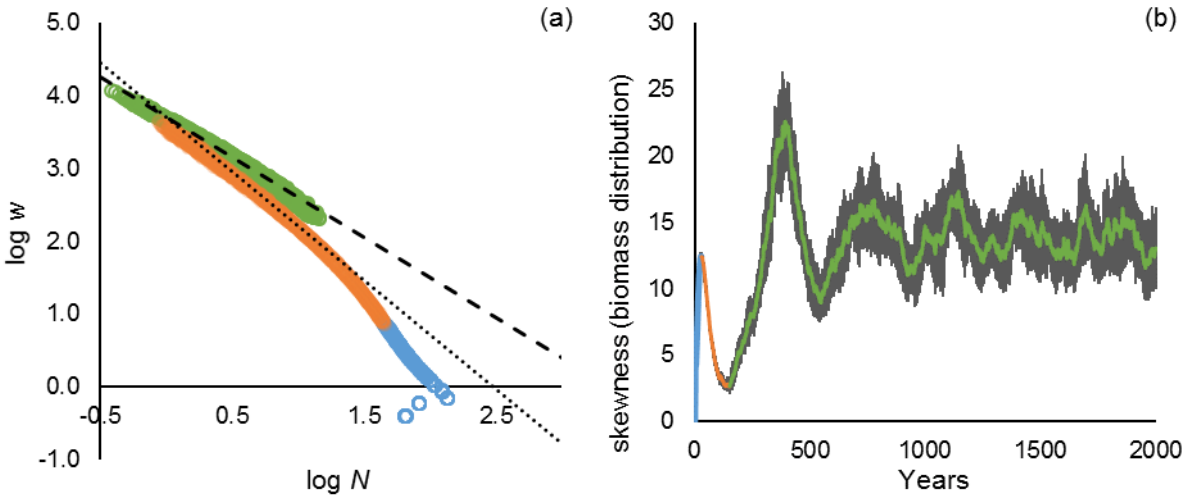

Figure A4.5. Soil water potential -80001, $f_d(\Psi) = 0.70$.

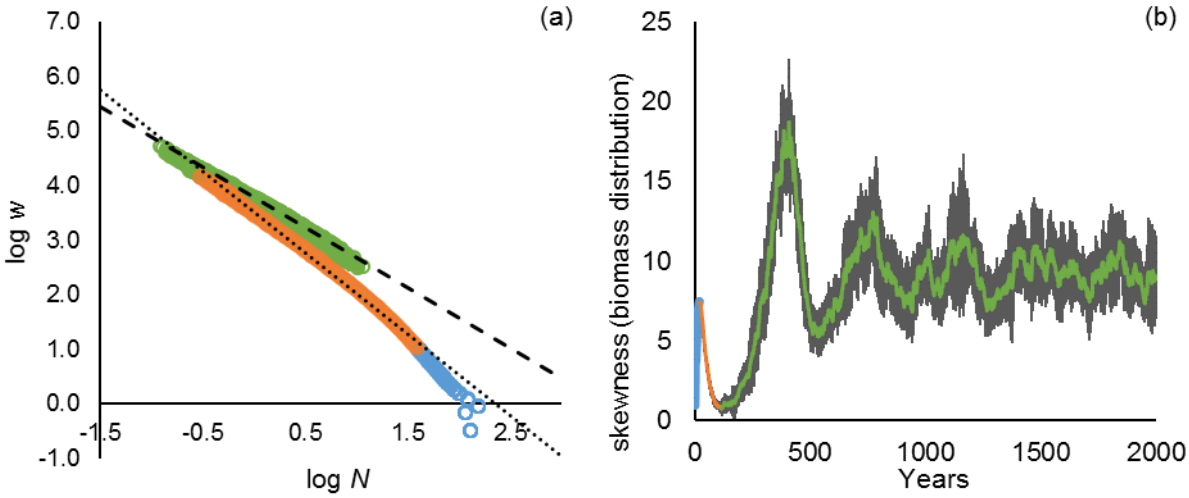

Figure A4.6. S Soil water potential -56000, $f_d(\Psi) = 0.80$.

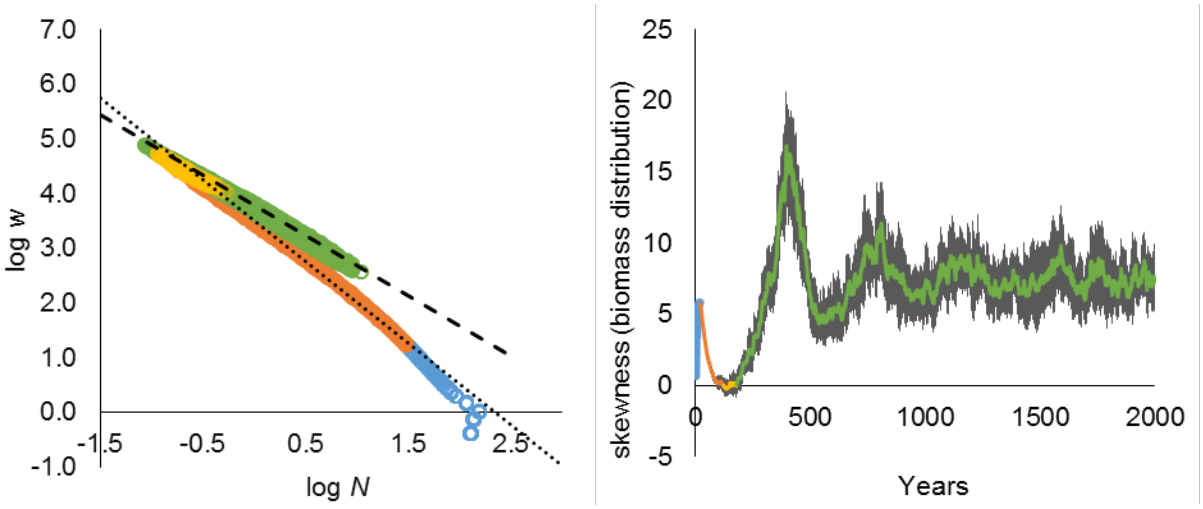

Figure A4.7. S Soil water potential -41000, $f_d(\Psi) = 0.90$.

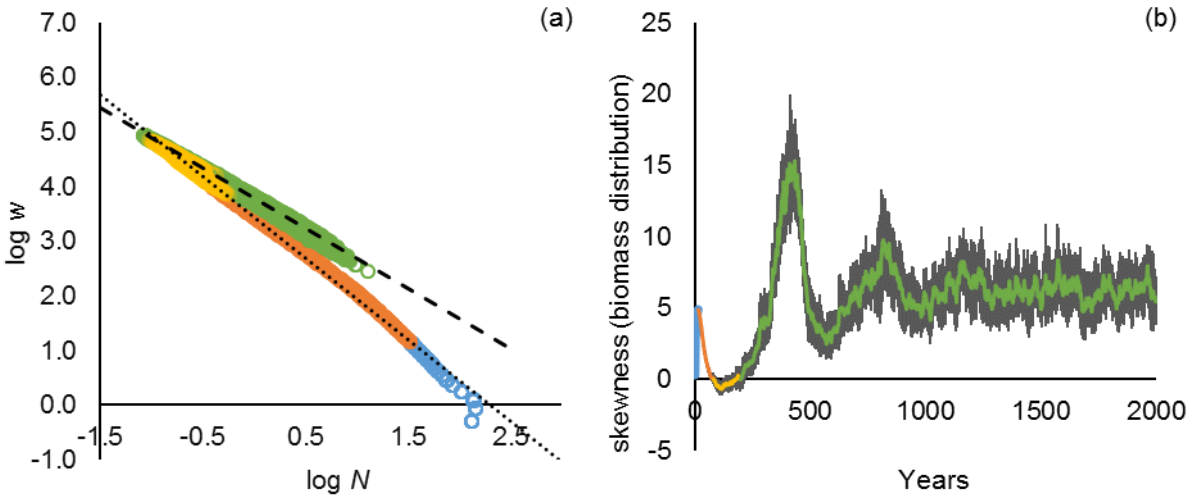

Figure A4.8. S Soil water potential -25400, $f_d(\Psi) = 0.93$.

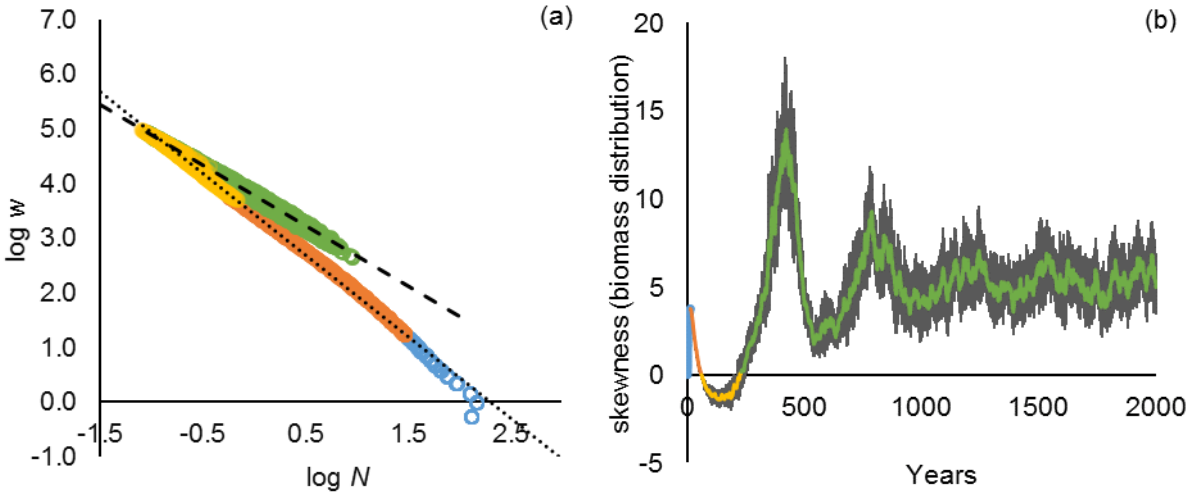

Figure A4.9. SSoil water potential -1900, $f_d(\Psi) = 1.00$.

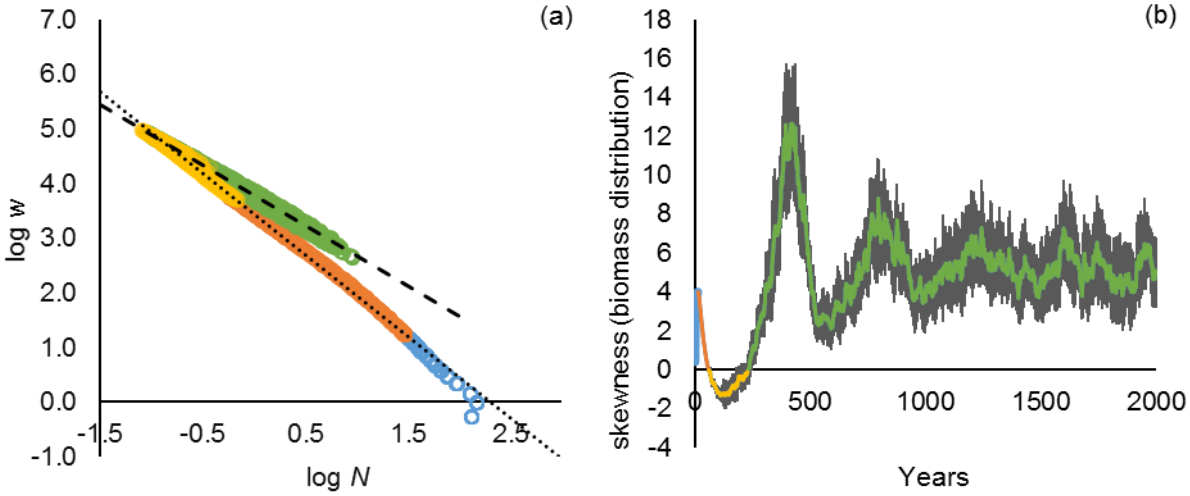

Figure A4.10. S Soil water potential -255, $f_d(\Psi) = 1.00$.

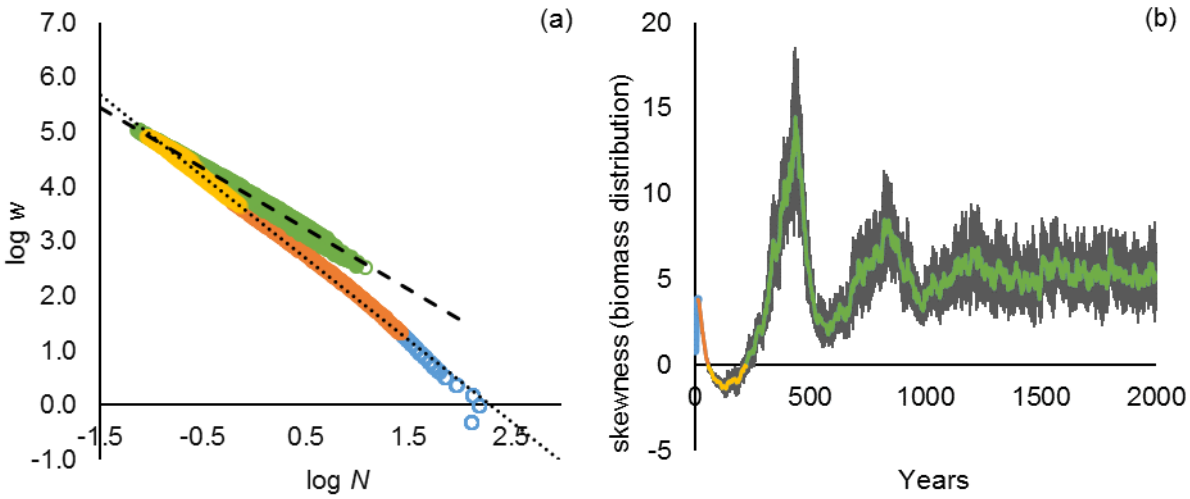

Figure A4.11. SSoil water potential -225, $f_d(\Psi) = 1.00$.

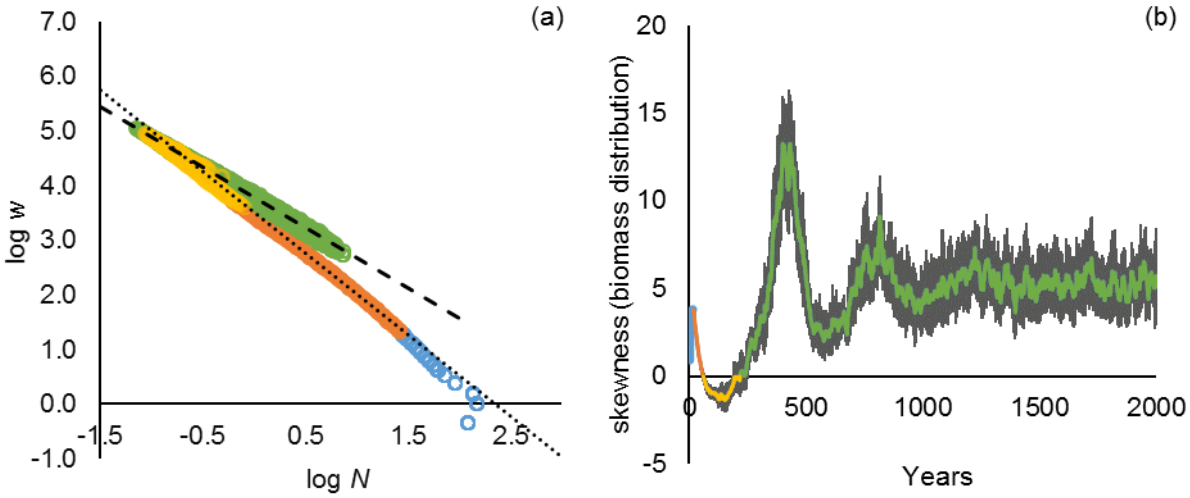

Figure A4.12. S Soil water potential -195, $f_d(\Psi) = 1.00$.

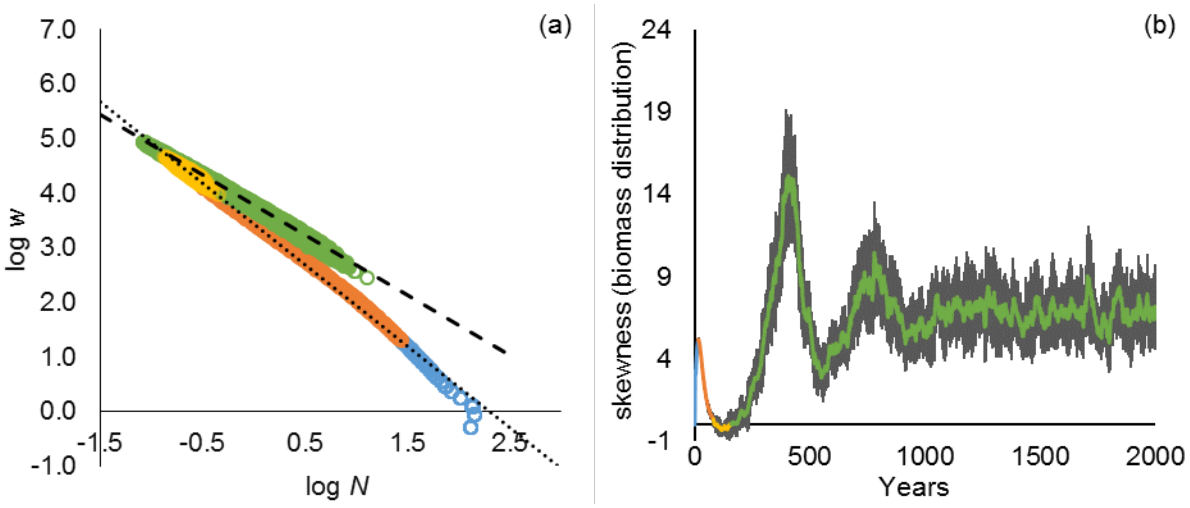

Figure A4.13. S Soil water potential -9.1, $f_d(\Psi) = 0.90$.

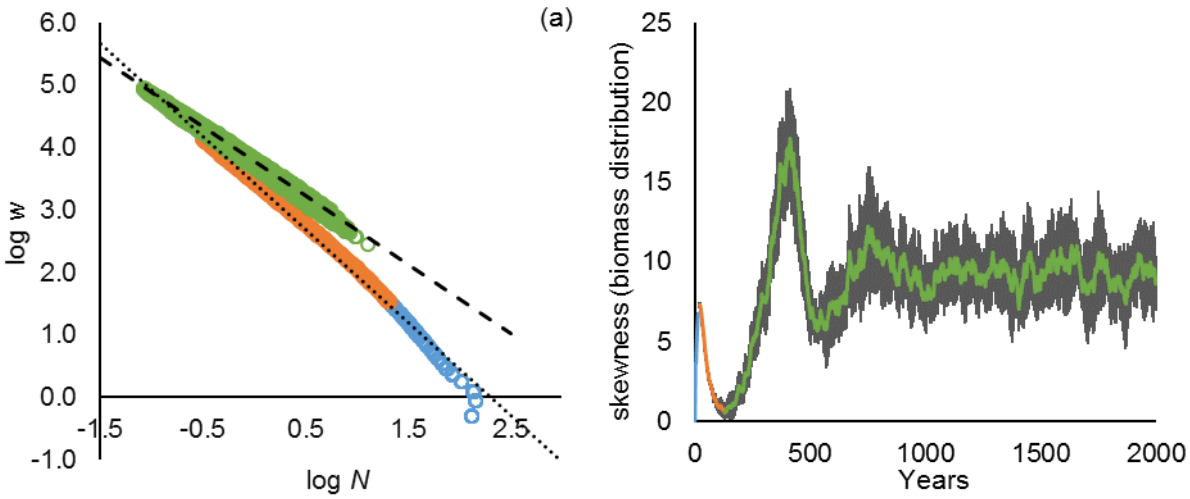

Figure A4.14. SSoil water potential -8.2, $f_d(\Psi) = 0.80$.

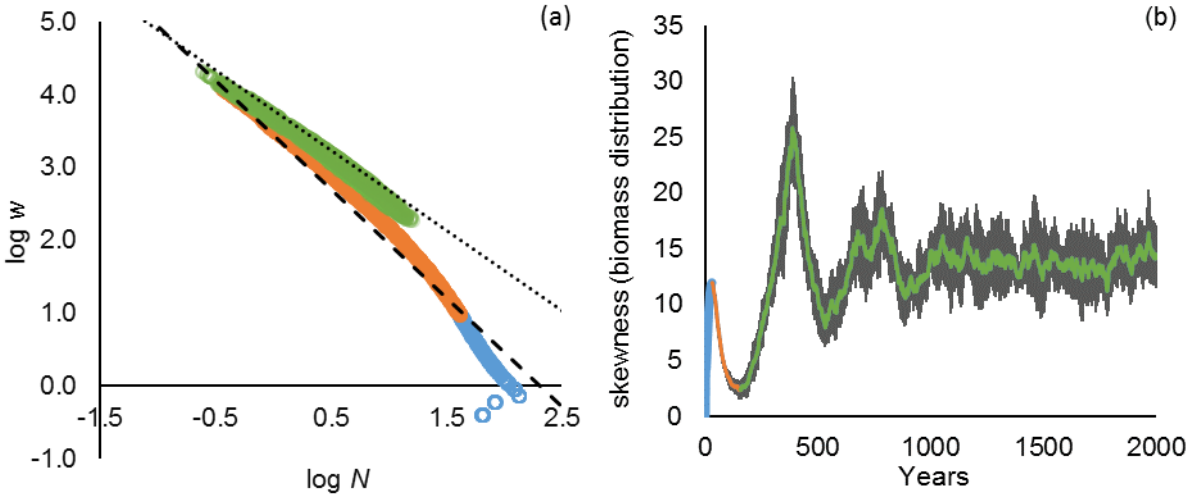

Figure A4.15. S Soil water potential -7.3, $f_d(\Psi) = 0.70$.

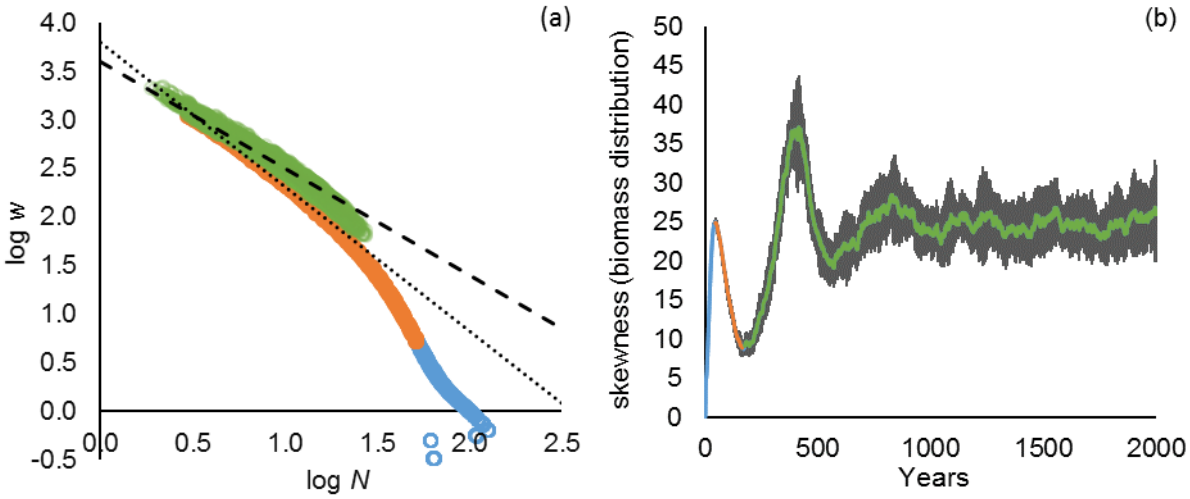

Figure A4.16. Soil water potential -6.4, $f_d(\Psi) = 0.60$.

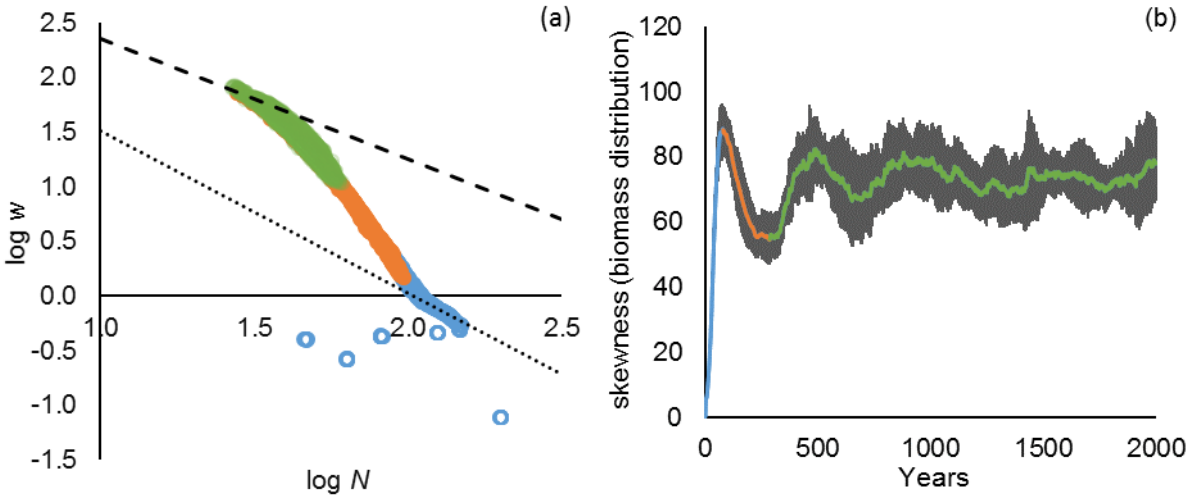

Figure A4.17. S Soil water potential -5.5, $f_d(\Psi) = 0.50$.

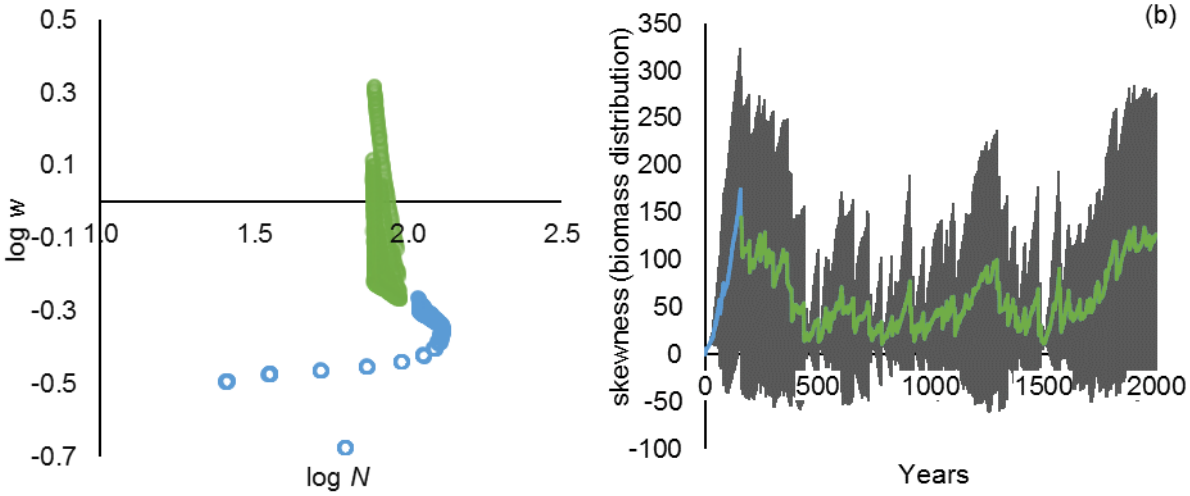

Figure A4.18. S Soil water potential -4.6, $f_d(\Psi) = 0.40$.

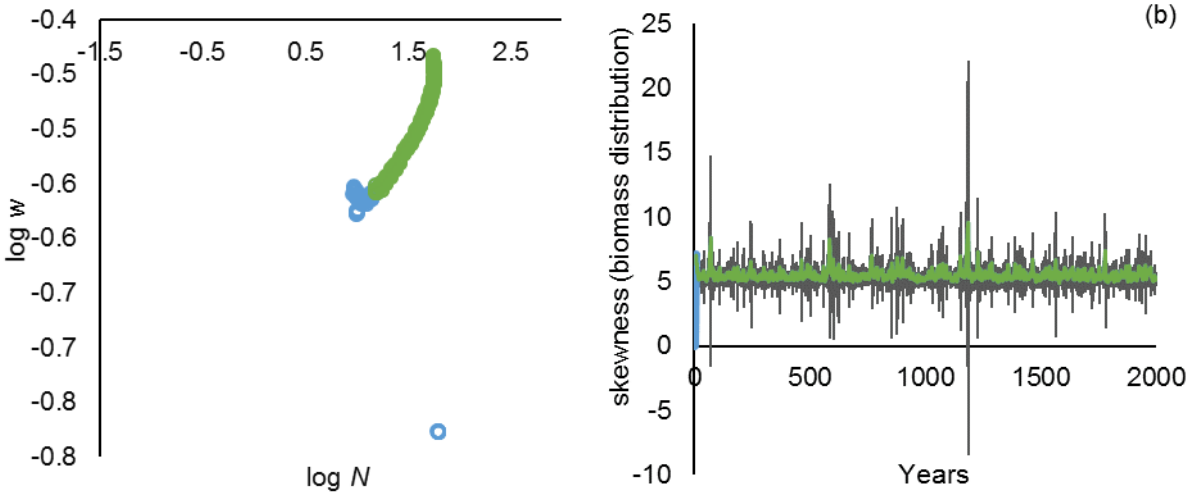

Figure A4.19. S Soil water potential -3.7, $f_d(\Psi) = 0.30$.

Appendix 5

Supplementary information on changes in community yield

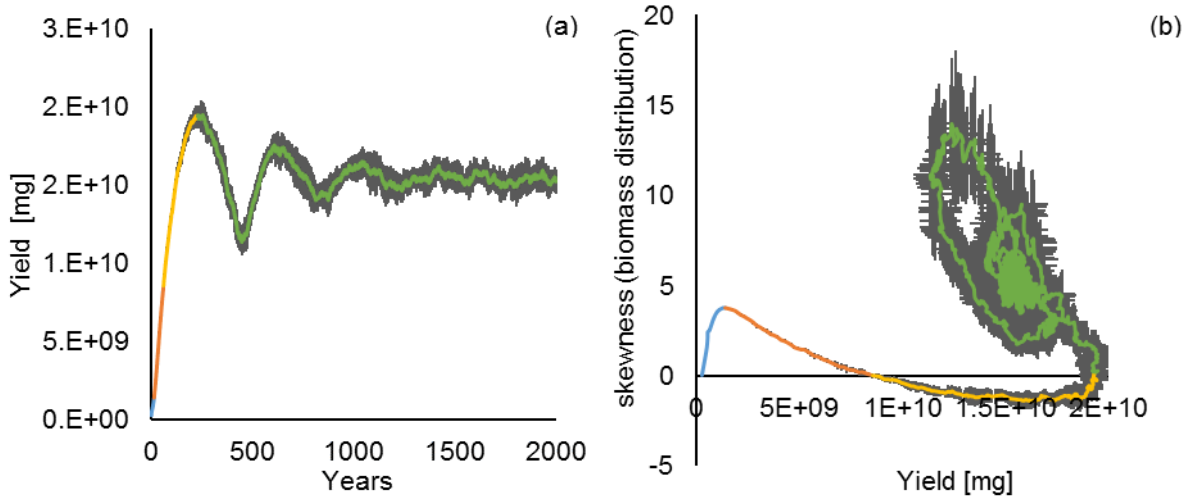

Figure A5.1. S Trajectory of the community yield [mg] of the base model scenario (soil water potential -1.9 E+3 mm, i.e. $f_T(\Psi) = 1.00$ and $f_t(\Psi) = 1.00$). Colors show the four sections of community structure indicated by skewness of the biomass distribution in Fig. 2. The standard deviation of the ten replicates is shown in grey. (a) Changes in mean ± SD community yield across all ten replicates over 2000 years. (b) Relationship between mean ± SD skewness of biomass distribution and mean ± SD community yield for all ten replicates over 2000 years.

Appendix 6

Biomass–density trajectories and skewness of the biomass distribution without recruitment

To highlight the prominent effect of recruitment on the biomass-density trajectories of the simulated plant communities, ten repetitions of the base model (Ψ = -1900 mm, i.e. the no PFT strategy experienced any stress) without recruitment were run. Therefore, the submodels '2.1.1.2 Seed survival in the seed bank', '2.1.1.3 Germination', '2.1.1.4 Seedling establishment', and '2.1.1.6 Seed production and dispersal' were switched of in PLANTHeR.

In these simulations the skewness of the biomass distributions as well as the biomass-density trajectories emerged in an almost textbook-like manner (Fig. A6.1) (Begon et al. 1991; Berger et al. 2002, Berger and Hildenbrandt 2003). The two x-intercepts and the first maximum of the skewness of the biomass distribution subdivided four distinct sections. In line with previous studies, section I was a fast growing section prior to self-thinning, i.e. only a few individuals were hindered in their growth such that they die at the end of this section (Begon et al. 1991). Section I was characterized by a decrease of negative skewness and ended with the first x-intercept. Bdts showed a non-linear relationship between log w and log N. Section I and II delineated the beginning and the end of the self-thinning process in the classical sense (Berger et al. 2002). Section II was characterized by an increase of positive skewness and ended with the maximum skewness. Section III exhibited a constant decay of positive skewness between the first maximum and the second x-intercept and corresponded to the classical thinning line (Berger et al. 2002). In section III, the fitted slopes were significantly flatter than the slope predicted by the self-thinning rule (one-sample $t(9) = 57.97$, $p < 0.001$) with a mean of -1.088 and 95% CI [-1.104 to -1.072]. This is in line with a previous study on monospecific even-aged populations which reported a thinning slope of -1.1 under size-symmetric competition for an unspecified resource (Lin et al. 2014). Section IV started at the second x-intercept with a negatively decreasing skewness. In this section, the bdts deviated from the linear thinning line because individuals of the initial cohort approached their maximum size (Berger et al. 2002). Therefore, mortality probability due to senescence increased and subsequently, increased the formation of gaps. As a consequence, in line with previous studies without recruitment, bdts bended below the thinning line and eventually ran parallel to the x-axis (Berger et al. 2002; Monserud et al. 2004).

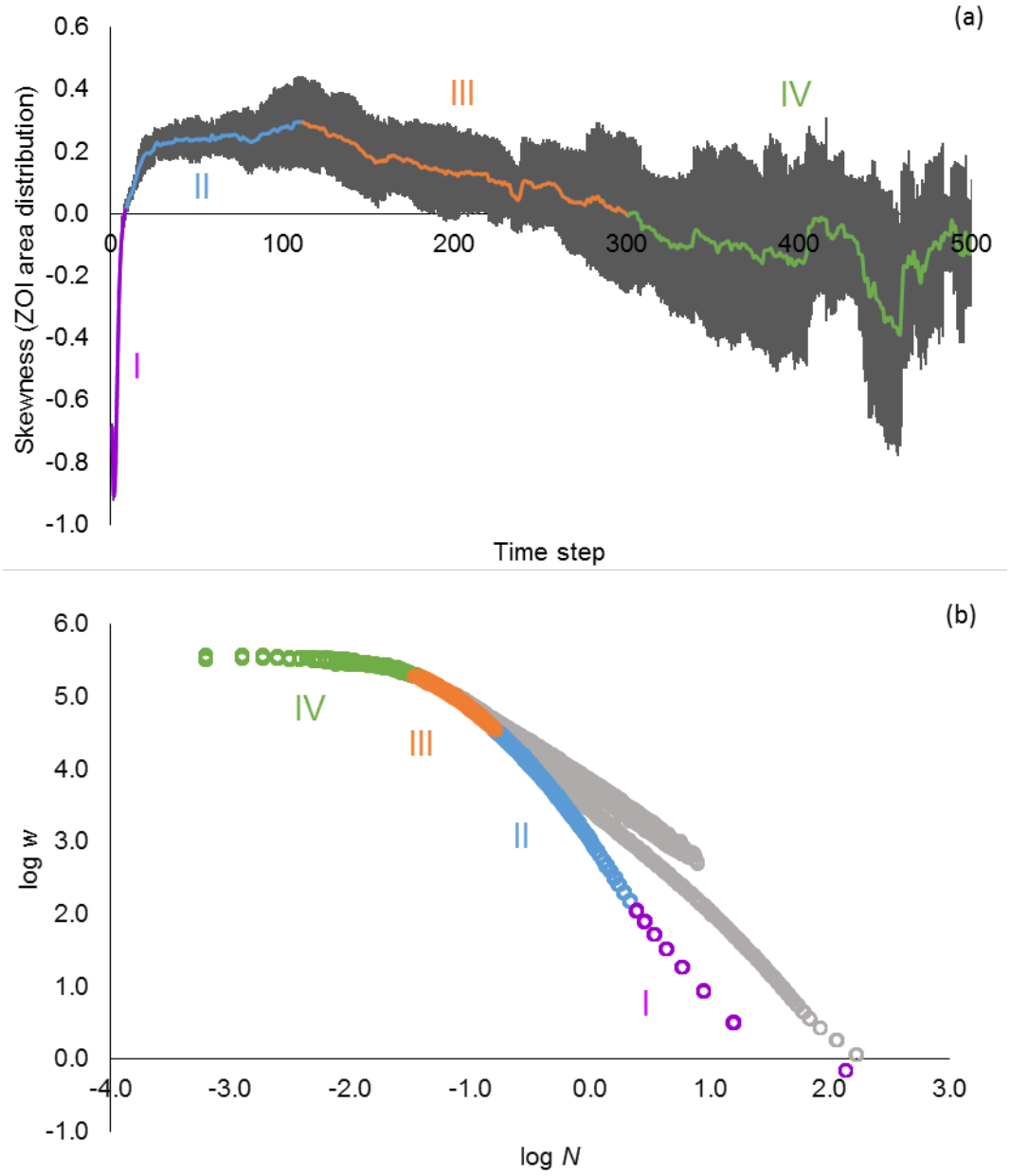

Figure A6.1 (a) Change in mean ± SD (in grey) skewness of the biomass distribution of the base model (Ψ = -1900 mm, i.e. the no PFT strategy experienced any stress) without recruitment across ten replicates over 2000 years. The two x-intercepts and the first maximum defined four distinct sections which are color-coded. (b) Entire biomass-density trajectory of the base model without any recruitment; i.e. relationship between the logarithm of mean plant biomass of survivors *w* (mg/m²) and the logarithm of plant density *N* (individuals/m²) for all ten replicates over 2000 years. Colors show the four sections of community structure indicated by the skewness of the biomass distribution in Fig. a. Grey dots in the background show the biomass-density trajectory of the base model including recruitment.

Appendix 7

Skewness of the age distribution for two exemplary soil water scenarios

Changes in the biomass-density trajectory over time can be tracked by means of the skewness of the biomass distribution (Berger et al. 2002). The skewness of the biomass distribution subdivided the biomass-density trajectory into maximum four distinct sections. Section I (blue) was characterized by an increase of positive skewness and ended with the first maximum of skewness. Section II (orange) was characterized by a constant decrease of positive skewness between the first maximum and the first x-intercept. Section III (yellow) was characterized by a negative skewness between the two x-intercepts. Section IV (green) started at the second x-intercept with an increasing positive skewness and was characterized by alternating phases of increasing and decreasing skewness. The changes of the skewness of the biomass distribution and the skewness of the age distribution were comparable over time in section II-IV.

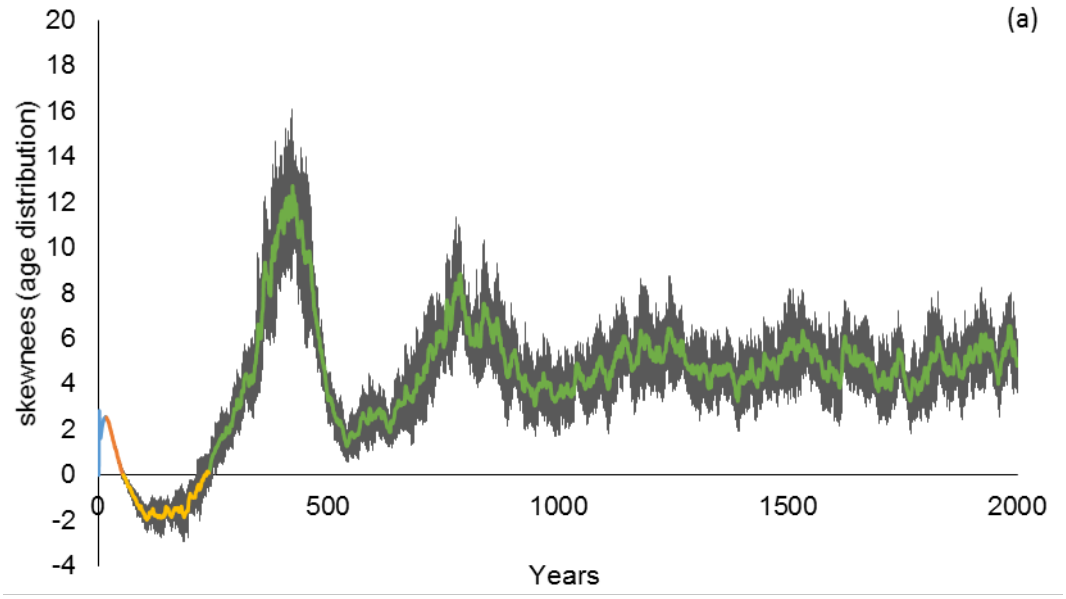

Figure A7.1. Change in mean ± SD (in grey) skewness of the age distribution across ten replicates over 2000 years for optimal soil water conditions (base model; Ψ = -1900 mm). The two x-intercepts and the first maximum defined four distinct sections (I to IV) which are color-coded as explained above.

References cited in the Appendix

Bakker, J. et al. 1996. Seed banks and seed dispersal: important topics in restoration ecology. - Acta Bot. Neerl. 45: 461-490.

Bauer, S. et al. 2002. Cyclic dynamics in simulated plant populations. - Proceedings of the Royal Society B: Biological Sciences 269: 2443-2450.

Bittner, S. et al. 2010. Modeling stand water budgets of mixed temperate broad-leaved forest stands by considering variations in species specific drought response. - Agric. For. Meteorol. 150: 1347-1357.

Caplat, P. and Anand, M. 2009. Effects of disturbance frequency, species traits and resprouting on directional succession in an individual-based model of forest dynamics. - J. Ecol. 97: 1028-1036.

Caplat, P. et al. 2008. Symmetric competition causes population oscillations in an individual-based model of forest dynamics. - Ecol. Modell. 211: 491-500.

Czárán, T. 1998. Spatiotemporal models of population and community dynamics. - Chapman and Hall.

DiVittorio, C. T. et al. 2007. Spatial and temporal patterns of seed dispersal: an important determinant of grassland invasion. - Ecol. Appl. 17: 311-316.

Feddes, R. et al. 1978. Simulation of field water use and crop yield. Simulation monographs. - Pudoc, Wageningen 189.

Grimm, V. et al. 2006. A standard protocol for describing individual-based and agent-based models. - Ecol. Modell. 198: 115-126.

Grimm, V. et al. 2010. The ODD protocol: A review and first update. - Ecol. Modell. 221: 2760-2768.

Herberich, M. M. et al. 2017. Hydrological niche segregation of plant functional traits in an individual-based model. - Ecol. Modell. 356: 14-24.

Jakobsson, A. and Eriksson, O. 2000. A comparative study of seed number, seed size, seedling size and recruitment in grassland plants. - Oikos 88: 494-502.

Levitt, J. 1980. Responses of Plants to Environmental Stresses: Water, Radiation, Salt, and Other Stresses. - Academic Press.

Roberts, E. 1972. Storage environment and the control of viability. Viability of seeds. Springer, pp. 14-58.

Schippers, P. et al. 2001. Herbaceous plant strategies in disturbed habitats : an evaluation using a spatially explicit model. - Oikos 95: 198-211.

Schulte, M. J. D. et al. 2013. Mode of competition for light and water amongst juvenile beech and spruce trees under ambient and elevated levels of O3 and CO2. - Trends Eco. Evol. 27: 1763-1773.

Seifan, M. et al. 2012. Combined disturbances and the role of their spatial and temporal properties in shaping community structure. - Perspect. Plant Ecol. Evol. Syst. 14: 217-229.

Seifan, M. et al. 2013. Beyond the Competition-Colonization Trade-Off: Linking Multiple Trait Response to Disturbance Characteristics. - Am. Nat. 181: 151-160.

Snyder, R. E. 2011. Leaving home ain't easy: non-local seed dispersal is only evolutionarily stable in highly unpredictable environments. - Proceedings of the Royal Society B: Biological Sciences 278: 739-744.

Stoyan, D. and Wagner, S. 2001. Estimating the fruit dispersion of anemochorous forest trees. - Ecol. Modell. 145: 35-47.

Weiner, J. and Damgaard, C. 2006. Size-asymmetric competition and size-asymmetric growth in a spatially explicit zone-of-influence model of plant competition. - Ecol. Res. 21: 707-712.

Weiner, J. et al. 2001. The Effects of Density, Spatial Pattern, and Competitive Symmetry on Size Variation in Simulated Plant Populations. - Am. Nat. 158: 438-450.

Wesseling, J. 1991. Meerjarige simulatie van grondwaterstroming voor verschillende bodemprofielen, grondwatertrappen en gewassen met het model SWATRE. - DLO-Staring Centrum.

Yang, S. J. and Jong, E. D. 1971. Effect of soil water potential and bulk density on water uptake patterns and resistance to flow of water in wheat plants. - Can. J. Soil Sci. 51: 211-220.